Formation of nanoscale liquid menisci in electric fields

Antonio Garcia-Martin and Ricardo Garcia[a)]
Instituto de Microelectrónica de Madrid, Consejo Superior de Investigaciones Cientificas, Isaac Newton 8, 28760 Tres Cantos, Madrid, Spain

(Received 10 October 2005; accepted 8 February 2006; published online 24 March 2006)

Nanometer-sized menisci of polar and nonpolar liquids are used to confine chemical reactions. Electric fields applied between two surfaces a few nanometers apart allow the formation and manipulation of three-dimensional nanoscale liquid bridges. At low fields, two stable shapes coexist: one represents a small liquid protrusion underneath the strongest field lines while the other is a nanoscale liquid contact bridging both surfaces. The formation of a nanoscale liquid meniscus requires the application of a threshold voltage to overcome the energy barrier between stable configurations. The bridge formation is accompanied by a drastic reduction of the electrical field at the solid-liquid interface. © *2006 American Institute of Physics*. [DOI: 10.1063/1.2189162]

Advances in nanoscale lithographies emphasize the relevance of manipulating very tiny liquid contacts. Those contacts serve as nanoscale reactors to confine different chemical reactions.[1–6] Pattern definition and performance of several nanoscale devices depend critically on the size of the water meniscus that confines the anodic oxidation.[7–10] Furthermore, field-induced force microscopy modification experiments with organic solvents depend either on the meniscus size[11] or on the field distribution within the liquid.[12,13] Different aspects of capillary formation in the macroscopic and microscopic domains have been recently described. Changes of the refractive index during the evaporation process have been associated with evolving density profiles.[14] Other studies have discovered several morphological wetting transitions on structured surfaces.[15] Even the dynamics of microscopic liquid bridges under the influence of external fields have been imaged by electron and optical microscopes.[16,17] It is recognized that electric fields offer the best approach to control and manipulate liquid bridges.[18] The spontaneous formation of nanoscale water bridges is a common phenomena whenever two surfaces brought into mechanical contact have nanometer-sized cracks or pores comparable to the Kelvin radius.[19] However, the reproducible formation of sub-50 nm liquid bridges is experimentally challenging, so studies of nanoscale menisci are still emerging.[20–22] Thus, the properties of genuinely nanoscale liquid bridges, i.e., those with a nanometer-sized volume, are usually extrapolated from macroscopic or microscopic studies. This is in stark contrast with the large body of studies dealing with the properties of solid-state nanocontacts.[23]

Here we describe the formation of nanoscale water and ethanol menisci between a sharp probe and a conductive surface in the presence of electric fields. The properties of the interface are controlled by the coexistence of two stable liquid shapes. One shape corresponds to the formation of a tiny liquid protrusion below the tip's apex while other is a liquid meniscus bridging tip and surface. The formation of a liquid bridge involves a sharp increase of the field of up 10 V/nm.

The experimental setup consists of an amplitude modulation atomic force microscope (AFM) operated in the noncontact regime.[24] The instrument is enclosed in a chamber filled with N_2 and vapors from either water or ethyl alcohol (CH_3CH_2OH). A voltage pulse applied between the tip and sample condenses the vapor underneath the AFM tip, which gives rise to the formation of a nanometer-size liquid bridge. Tip-surface separation, voltage strength, and pulse duration controls the meniscus size. We have used *p*-type Si(100) surfaces with a resistivity of 0.1–1.4 Ω cm and *n*-doped silicon cantilevers with force constants of 30 and 36 N/m for water and ethanol, respectively. The average tip-surface distance is measured by recording simultaneously the dependence of the amplitude and the cantilever's deflection as a function of the *z*-piezo displacement. The minimum in the deflection curve establishes the origin of the average distance. This method ignores any tip-surface deformation.

The formation of either a water or an ethanol meniscus as a function of the voltage is determined by detecting the effect of the meniscus capillary force on the tip. Those effects become evident by following the dynamics of the tip's oscillation before, during, and after the application of a voltage pulse.[8] When the pulse is on the electric field deflects the mean position of the tip and reduces its oscillation amplitude. The signature of the formation of a liquid bridge is that, after turning the pulse off, the amplitude remains reduced and the tip mean position is slightly deflected towards the surface. In the absence of a liquid meniscus, the amplitude recovers in $QT/\pi \sim 1$ ms and no deflection is observed.

The size of ethanol and water bridges can be obtained by measuring the snap-off distance of the bridges. Its size depends on tip-surface separation, relative humidity, tip radius, and applied voltage. Here, we have formed water and ethanol bridges of diameters (at waist) and lengths in the 20–40 and 4–12 nm ranges, respectively.

The total energy involved in the formation of nanometer-size liquid bridges in electric fields has contributions from surface (U_S), condensation (U_C), van der Waals (U_{vdW}), and electrostatic (U_E). The experimental AFM interface is modeled by a sharp tip with an ideal parabolic shape and a flat surface with a thin liquid film adsorbed on it. This interface implies the nonlocal character of the electrical field, which in turn makes electrostatic calculations rather difficult and cumbersome.[25,26] To provide a realistic description, as well as to give general analytical expressions that relate the relevant physical parameters, we have introduced some approximations in the shape of the liquid protrusion induced by

[a)]Electronic mail: rgarcia@imm.cnm.csic.es

the field. The shape is described by a hyperbolic function that has radial symmetry ρ and is parametrized by its height at its maximum (h) and by its width (w) at half-maximum:

$$\xi(\rho) = h_0 + \frac{h}{\cosh(\rho/w)}. \tag{1}$$

This expression reproduces the shape of the protrusions obtained by numerical simulations. The actual shape of the protrusion for a given geometry and bias voltage is described by the set $\{h,w\}$ that minimizes the total energy. Using this parametrization the different energy terms are expressed as differences between relaxed and unrelaxed interface energies:

$$\Delta U_S = 2\pi\gamma \int_0^\infty \rho(\sqrt{1+\xi'^2} - 1)d\rho, \tag{2}$$

$$\Delta U_C = \frac{2\pi RT}{v_m} \ln\left(\frac{1}{H}\right) \int_0^\infty \rho(\xi - h_0)d\rho, \tag{3}$$

$$\Delta U_{\mathrm{VdW}} = \frac{h_0^3 \pi RT}{v_m} \ln\left(\frac{1}{H}\right) \int_0^\infty \rho\left(\frac{1}{\xi^2} - \frac{1}{h_0^2}\right)d\rho, \tag{4}$$

where γ is the liquid-vapor surface energy, $R = 8.31\ \mathrm{J\ mol^{-1}\ K^{-1}}$, T is the temperature, v_m is the molar volume, H is the relative humidity, h_0 is the height of the liquid film on the surface when there is no applied bias voltage,[27] and h_0 depends on the Hamaker constant.

The electrostatic energy is calculated within the radial field approximation,

$$\Delta U_E = -\pi\varepsilon_0\varepsilon V^2 \int_0^{\pi/2} \sin\theta G(R_M, R_m, R_{\mathrm{tip}}, R_w)d\theta, \tag{5}$$

where G is a geometrical factor that depends on the different radii of the interface.[28]

Since during the pulse application the cantilever is deflected towards the surface, the tip-surface separation is thus being modified. In order to take this effect into account we have to find the equilibrium position for a given bias voltage and cantilever parameters. The balance between the electrostatic force and the restoring elastic cantilever force can be expressed as $F_E \approx \pi\varepsilon_0\varepsilon V^2(R_{\mathrm{tip}}/D + C) = k(D-d)$,[29] where C is a constant that depends on the actual tip shape and it is determined from experimental data.

Figure 1 shows the energy curves ΔU (=energy of the relaxed surface-energy of the unrelaxed surface) of water as a function of the height of the protrusion for several applied voltages. For low voltages, the interface is characterized by a *monostable* regime. The total energy has a minimum very close to the sample surface. This minimum corresponds to the formation of a very small protrusion of the liquid film (<0.1 nm) underneath the strongest field lines. At some intermediate voltages ($\sim 5-11.2$ V for water with $D=6$ nm and $R_{\mathrm{tip}}=30$ nm), the energy has two minima with respect to w and h. The *bistable* regime has a local minimum close to the surface and an absolute minimum where the liquid fills the tip-surface gap [Fig. 1(a)]. By increasing the voltage, the local minimum decreases and eventually disappears. Then another monostable configuration is reached. Here a liquid meniscus bridges the gap between tip and surface. The existence of monostable and bistable regimes implies two characteristic voltages. From low to high voltages, V_m marks the transition from the monostable to the bistable regime, and a threshold voltage V_{th} the transition from the bistable to the upper monostable regime. V_m is the minimum voltage that sustains a liquid bridge.

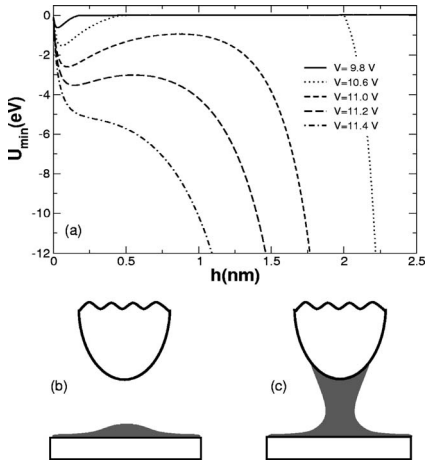

FIG. 1. (a) Energy curves for several applied voltages as a function of the height of the liquid protrusion (water). For low voltages the energy curve shows a minimum very close to the sample surface. Above a certain critical voltage the curve shows two minima. A local minimum close to the surface and an absolute minimum where the liquid fills the tip-surface gap. By increasing the voltage the local minima disappears. Average tip-surface separation $D=6$ nm and $H=0.37$. Schematic representation (not to scale) of the geometry of the interface associated with (b) the first local minimum (protrusion) and (c) the absolute minimum (liquid bridge).

The coexistence of two shapes for some voltages and distances and the activation barrier that separates them introduces a history dependent final shape. Initially, the liquid bridge is only formed for voltages above the threshold value. But the bistable regime implies that once the liquid bridge has been formed, the voltage could be lowered to voltages slightly above V_m without evaporating the bridge.

The electric fields associated with each shape in the bistable regime are quite different (Fig. 2). Electrical fields are calculated at the sample solid-liquid interface. The formation of a liquid meniscus implies a remarkable increase of the electric field up to 10 V/nm at the flat surface. Those values are approximately 50 (water) and 15 (ethanol) times higher than those calculated in the presence of a liquid protrusion. Higher values are obtained for water because $\varepsilon_{\mathrm{water}} > \varepsilon_{\mathrm{eth}}$. Nonetheless, the fields associated with the liquid

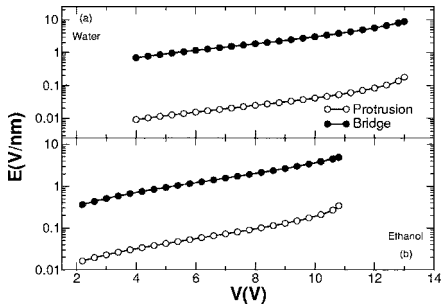

FIG. 2. Electric field dependence on the liquid shape (bistable regime). (a) Water, $H=0.30$ and (b) ethanol, $H=0.6$. Tip radius $R=30$ nm. Open symbols are for the liquid protrusion while filled symbols are for a liquid bridge. Fields are 10–100 times higher in the presence of a meniscus because the dielectric constants of liquids are higher than the dielectric constant of air. The fields are calculated at the sample's solid-liquid interface just under the tip's apex.

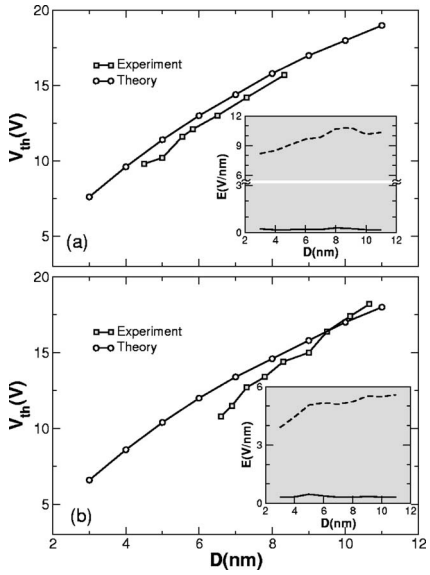

FIG. 3. Experiment and theory threshold voltage dependence on tip-surface separation. (a) Water, $H=0.30$ and (b) ethanol, $H=0.6$. Tip radius $R=30$ nm. The inset shows the dependence of the maximum electric field on tip-surface separation just before (solid line) and after (dotted line) the meniscus formation.

bridge are below the values needed for field ionization[30] ($\sim$25–50 V/nm), so the formation of a liquid bridge by itself does not involve any modification of the surface.

The disappearance of the local minimum in the energy curves as the voltage is increased can be directly related to the experimental observation of the existence of a threshold voltage for the formation of a liquid nanocontact bridging tip and sample surface. In Fig. 3 we plot the comparison between theory and experiment for the formation of water and ethanol nanoscale liquid bridges. The dependence of the threshold voltage as a function of the average tip-surface separation shows a remarkable agreement for both liquids. The threshold voltage increases monotonically with the average tip-surface separation in both cases. For the same tip-surface separation, the formation of nanoscale water bridges requires slightly higher voltages because condensation $[\nu_m(\text{water}) < \nu_m(\text{eth})]$ and surface energies ($\gamma_{\text{eth}} < \gamma_{\text{water}}$) are larger for water. Those effects offset the influence of the dielectric constant in the electrostatic force ($\varepsilon_{\text{water}} > \varepsilon_{\text{eth}}$) [Eq. (5)].

The dependence of the maximum electric field at the silicon surface is depicted in the insets. Two fields are calculated, the electric field for a bias just below V_{th} (solid line) and the field for a voltage just above V_{th} (discontinuous line). Electric fields are one to two orders of magnitude smaller when the interface is characterized by a small liquid protrusion underneath the tip's apex than when the tip surface gap is filled by a nanoscale liquid contact.

The shapes of the bistable regime depicted in Figs. 1(b) and 1(c) have both different properties and formation mechanisms. The tiny protrusion formed underneath the tip's apex is mostly due to field-induced polarization of the adsorbed liquid film, while the liquid bridge comes mostly from the condensation of molecules in the vapor phase. Furthermore, the liquid protrusion amounts to a negligible number of molecules with respect to the liquid bridge. Nonetheless, it is the very coexistence of those two shapes that controls the size of the liquid bridge. The coexistence introduces a history dependent final shape that allows us to have a stable liquid bridge below the threshold voltage. Because the meniscus size depends on the applied voltage, the bistable regime provides a protocol to control and, in particular, to decrease the meniscus size by decreasing the voltage to values slightly above the minimum voltage that sustains a liquid bridge. The energy dependence of the two shapes with the voltage gives rise to three regimes, two associated with each shape and the other associated with the coexistence of the two.

The authors thank Marta Tello and Juan José Sáenz for fruitful discussions. This project was funded by MCyT (Spain) under Contract No. MAT2003-02655 and by the European Commission project NAIMO IP 500355-2. A.G.-M. acknowledges financial support from the Spanish MEC through its Ramón y Cajal program.

[1] M. Cavallini and F. Biscarini, Nano Lett. **3**, 1269 (2003).
[2] S. Hoeppener, R. Maoz, and J. Sagiv, Nano Lett. **3**, 761 (2003).
[3] S. F. Lyuksyutov, R. A. Vaia, P. B. Paramonov, S. Juhl, L. Waterhouse, R. M. Ralich, G. Sigalov, and E. Sancaktar, Nat. Mater. **2**, 468 (2003).
[4] B. W. Maynor, J. Y. Li, C. G. Lu, and J. Liu, J. Am. Chem. Soc. **126**, 6409 (2004).
[5] D. Wouters and U. S. Schubert, Angew. Chem., Int. Ed. **43**, 2480 (2004).
[6] M. Tello, R. Garcia, J. A. Martín-Gago, N. F. Martinez, M. S. Martín-Gonzalez, L. Aballe, A. Baranov, and L. Gregoratti, Adv. Mater. (Weinheim, Ger.) **17**, 1480 (2005).
[7] A. Fuhrer, S. Luescher, T. Ihn, T. Heinzel, K. Ensslin, W. Wegscheider, and M. Bichler, Nature (London) **413**, 822 (2001).
[8] M. Calleja, M. Tello, and R. Garcia, J. Appl. Phys. **92**, 5539 (2002).
[9] J. A. Dagata, F. Perez-Murano, C. Martín, H. Kuramochi, and H. Yokoyama, J. Appl. Phys. **96**, 2393 (2004).
[10] C. F. Chen, S. D. Tzeng, H. Y. Chen, and S. Gwo, Opt. Lett. **30**, 652 (2005).
[11] R. V. Martinez and R. Garcia, Nano Lett. **5**, 1161 (2005).
[12] C. R. Kinser, M. J. Schmitz, and M. C. Hersam, Nano Lett. **5**, 91 (2005).
[13] I. Suez, M. Rolandi, and J. M. Frechet, Nano Lett. **5**, 321 (2005).
[14] N. Maeda, J. N. Israelachvili, and M. M. Kohonen, Proc. Natl. Acad. Sci. U.S.A. **100**, 803 (2003).
[15] R. Seemann, M. Brinkmann, E. J. Kramer, F. F. Lange, and R. Lipowsky, Proc. Natl. Acad. Sci. U.S.A. **102**, 1848 (2005).
[16] M. Schenk, M. Futing, and R. Reichelt, J. Appl. Phys. **84**, 4880 (1998).
[17] A. Klingner, S. Herminghaus, and F. Mugele, Appl. Phys. Lett. **82**, 4187 (2003).
[18] C. Quilliet and B. Berge, Curr. Opin. Colloid Interface Sci. **6**, 34 (2001).
[19] J. Israelachvili, *Intermolecular and Surface Forces* (Academic, London, 1992).
[20] W. J. Stroud, J. E. Curry, and J. H. Cushman, Langmuir **17**, 688 (2001).
[21] S. Gomez-Moñivas, J. J. Saenz, M. Calleja, and R. Garcia, Phys. Rev. Lett. **91**, 056101 (2003).
[22] J. K. Jang, G. C. Schatz, and M. A. Ratner, J. Chem. Phys. **120**, 1157 (2004).
[23] N. Agrait, A. L. Yeyati, and J. M. van Ruitenbeek, Phys. Rep. **377**, 81 (2003).
[24] R. Garcia and A. San Paulo, Phys. Rev. B **60**, 4961 (1999).
[25] G. Mesa, E. Dobado-Fuentes, and J. J. Saenz, J. Appl. Phys. **79**, 39 (1996).
[26] S. Kremmer, S. Peisel, C. Teichert, F. Kuchar, and H. Hofer, Mater. Sci. Eng., B **102**, 88 (2003).
[27] G. E. Ewing, J. Phys. Chem. **108**, 15953 (2004).
[28] $G=\{R_{\text{tip}}R_MR_m/[R_M\varepsilon(R_m-R_{\text{tip}})+R_{\text{tip}}(R_M-R_m)]\}-\{R_{\text{tip}}R_MR_\omega/[R_M\varepsilon(R_w-R_{\text{tip}})+R_{\text{tip}}(R_M-R_w)]\}$ where $R_M=(R_{\text{tip}}+D)/\cos\theta$, $R_m=(R_{\text{tip}}+D-\xi)/\cos\theta$, $R_w=(R_{\text{tip}}+D-h_0)/\cos\theta$, and $h_0^3=(|A|/6\pi)\times[(RT/v_m)\ln(1/H)]^{-1}$. $\gamma(\text{water})=73$ mJ/m^2, $\gamma(\text{ethanol})=23$ mJ/m^2; $v_m(\text{water})=18\times10^{-6}$ m^3/mol, $v_m(\text{ethanol})=58\times10^{-6}$ m^3/mol; $A=37\times10^{-20}$ J m; $\varepsilon(\text{water})=79$, $\varepsilon(\text{ethanol})=24$.
[29] H. W. Hao, A. M. Baró, and J. J. Sáenz, J. Vac. Sci. Technol. B **9**, 1323 (1991).
[30] R. Gomer, *Field Emission and Field Ionization* (American Institute of Physics, New York, 1993).